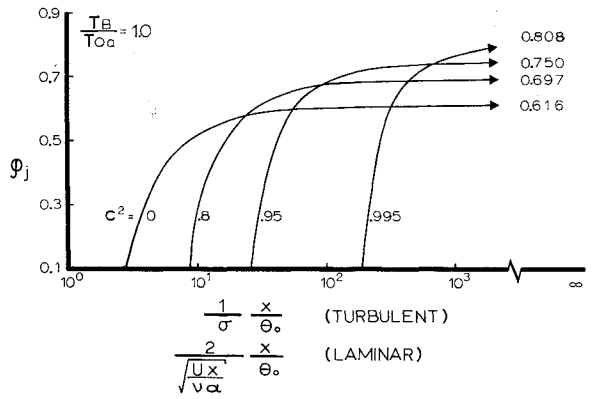

Fig. 1 Dimensionless velocity of dividing streamline for half-infinite isoenergetic jet mixing of a perfect gas.

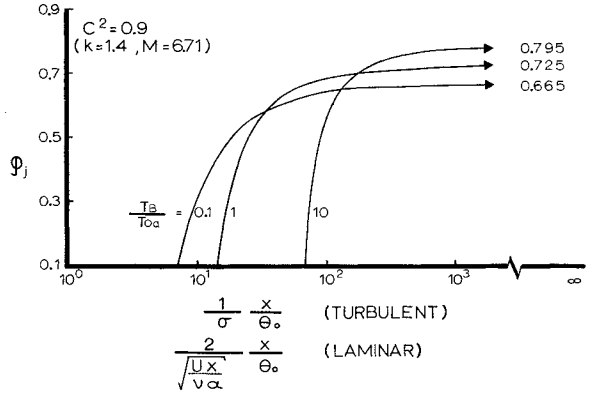

Fig. 2 Dimensionless velocity of dividing streamline for half-infinite diabatic jet mixing of a perfect gas.

either a laminar or turbulent abscissa for an adiabatic two-dimensional mixing region with the square of the Crocco number (U/U_{max}) of the adjacent flow as a parameter. (The equivalent mass bleed concept[4,5] was used for the calculations.) Regardless of the character of the flow, the abscissa is a measure of the length of the mixing region x in terms of the momentum thickness at the start of the mixing region θ_0. The limiting values of φ_j for fully developed mixing are also shown. As shown, smaller values of φ_j are obtained for developing mixing regions (i.e., those with initial boundary layers of finite thickness as compared with wake length).

Figure 2 shows an example with heat transfer for a perfect gas with Prandtl number of unity. It shows that the diabatic condition influences φ_j for the laminar and turbulent cases. The ratio of bulk temperature of the stagnant gas T_B to the total temperature of the adjacent flow T_{0a} is an important parameter.

In order to obtain numerical results from Figs. 1 and 2, α must be known. The integral method from which these two figures were obtained uses an error function solution of a simplified equation of motion to approximate the velocity profile appearing in the integrals. The simplified equation of motion may be obtained by a perturbation procedure from the boundary-layer equation of motion. If the procedure uses perturbations about the potential velocity $\alpha = 1.0$, and if about the average mixing region velocity, $\alpha = 2.0$. Although there are some indications[6] that α tends toward 2.0, further evidence is needed in order to determine α precisely.

Even without precise knowledge of α, Figs. 1 and 2 indicate an example of the usefulness of this turbulent-to-laminar transformation for adiabatic and diabatic mixing regions.

References

[1] Bhuta, P. G. and Page, R. H., "Nonsteady two-dimensional laminar and turbulent jet mixing theory," *Proceedings of the 4th U.S. National Congress of Applied Mechanics* (American Society of Mechanical Engineers, New York, 1962), pp. 1205–1212.

[2] Korst, H. H., Chow, W. L., and Zumwalt, G. W., "Final report on research in transonic and supersonic flow of a real fluid at abrupt increases in cross section," Univ. of Illinois, ME-TR-392-5, OSR-TR-60-74 (1959).

[3] Page, R. H., "On turbulent supersonic diabatic wakes," ARS J. 29, 443–445 (1959).

[4] Carriere, P. and Sirieix, M., "Facteurs d'influence du recollement d'un ecoulement supersonique," Office Nationale d'Etudes et de Recherches Aeronautiques, Memo. Tech. 20 (1961).

[5] Golik, R. J., "On dissipative mechanisms within separated flow regions," Ph.D. Thesis, Mechanical Engineering Dept., Univ. of Illinois (1962).

[6] Nash, J. F., "Laminar mixing of a non-uniform stream with a fluid at rest," Aero. Research Council Rept. 22,245, F.M. 3005 (September 1960).

Hypersonic Cone Wake Velocities Obtained from Streak Pictures

W. K. Washburn,* A. Goldburg,† and B. W. Melcher II‡

Avco-Everett Research Laboratory, Everett, Mass.

THE deceleration of the flow in the turbulent wake of hypersonic conical bodies has been investigated and reported by several authors.[1, 2] Slattery and Clay[1] obtained experimentally average velocities in cone wakes by following the histories of identifiable packages of gas at the edge of the turbulent front in high-speed schlieren moving pictures. Their data were resolvable starting at approximately 50 body diameters behind the cone and extended to some 3000 diameters downstream. Hromas and Lees[2] and Lien, Erdos, and Pallone[4] have calculated centerline velocities in cone wakes. These solutions cover the distance from the body to several hundreds of body diameters downstream.

For cone wakes, the region of maximum interest is near to the body because the disturbances in velocity and enthalpy produced by the cone are small, and these properties decay rapidly toward their freestream values under the influence of turbulent diffusion. For hypersonic conical flow fields, the maximum decay region for these properties is well within 25 body diameters for most cases of interest. By the streak drum camera technique,[5] it is possible to obtain data on representative cone wake velocities in the turbulent core in the important region between 5 and 25 diameters behind the body.

The cone wake velocity data in this paper were obtained from drum-camera streak photographs taken during experiments performed on Canadian Armament Research and Development Establishment (CARDE) Range 2. The projectiles were sharp 15° semivertex angle (θ_c) plastic (zelux) cones with base diameter equal to $\frac{1}{2}$ in. (One set of data was also obtained for a 45° semivertex angle cone.) Ranges of freestream properties from 0.88 to 7.6 cm Hg in pressure and from 14,000 to 16,000 fps in velocity were covered. A typical cone streak picture is shown in Fig. 1. The bright band was produced by the cone itself. The streaks, from which the wake velocity was measured, represent a flow unsteadiness.[7, 8] These disturbances are made visible by the self-luminosity of

Received March 24, 1964. The authors wish to thank the Canadian Armament Research and Development Establishment for the cooperative use of their ballistic range. The authors also wish to thank H. Lien and A. Pallone of Avco/RAD and L. A. Hromas and W. H. Webb of Space Technology Laboratories for kindly providing the turbulent wake solution for the correlations corresponding to the experiment.

* Senior Engineer. Member AIAA.

† Principal Research Scientist. Associate Fellow Member AIAA.

‡ Now at National Engineering Science Company, Pasadena, Calif. Member AIAA.

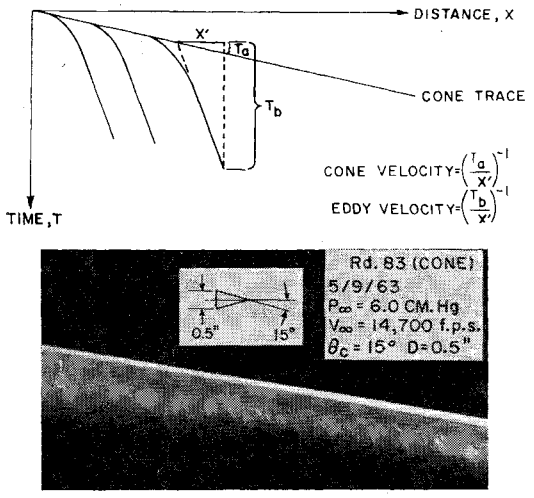

Fig. 1 Typical cone streak photograph showing streaks from which wake velocity information is derived. These data were obtained at the Canadian Armament Research and Development Establishment.

the ablation products produced in the cone boundary layer which trail back into the boundary-layer-induced wake (viscous core). It appears from the pictures that, as the boundary layer flows around and expands into the base region, the gas cools, suppressing the luminosity. Subsequently, through recompression and/or wake chemistry, the luminosity of the flow returns and traces out the average x-t histories of packages of the gas in the viscous core for several tens of body diameters.

Wake velocities are obtained by graphically taking the derivative of the x-t paths represented by a number of the streaks such as are shown in Fig. 1. This same technique was used by Hidalgo, Taylor, and Keck[5] to obtain wake velocities behind hypervelocity spheres. Figure 2 shows the results of such an analysis for the streaks of Fig. 1. The data points shown here have been fitted with a quartic curve fit. The root-mean-square deviation of the data distribution about the curve fit is noted on the figure.

Figure 3 shows the curve fit to the velocity data derived from three separate runs at a freestream pressure of $p_\infty = 6.0$ cm Hg. For the body size of these tests, $d_{base} = \frac{1}{2}$ in., and the velocities in the region of 15,000 fps, this pressure is almost an order of magnitude above the pressure at which unsteadiness first appears in the cone wake.[8]

The unsteady structure that is observed by the present technique is large scale. Fay and Goldburg[7] have shown that the growth of an unsteady wake that is dominated by large-scale structure is similar to that observed and predicted for the wake of small-scale well-mixed turbulence. (See their discussion with respect to their Fig. 20.) Since physical growth and velocity decay for the turbulent wake are controlled by the same physical phenomena, it is felt to be appropriate to compare the results of the present experiment

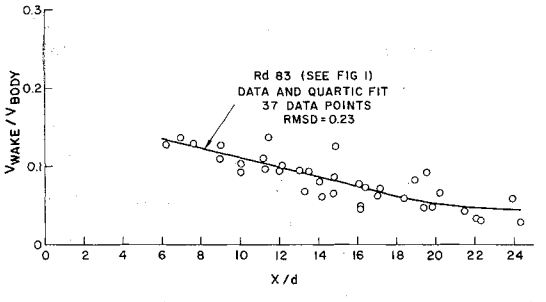

Fig. 2 Plot of velocity data obtained from streaks in Fig. 1. All velocities are measured in a coordinate system fixed in the laboratory.

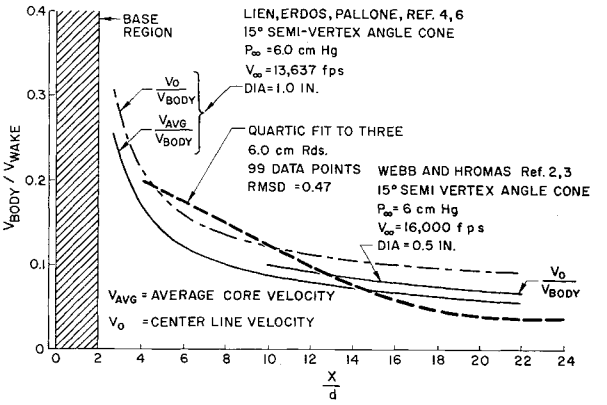

Fig. 3 Cone wake velocity data for 15° semivertex angle cones; $d_{base} = \frac{1}{2}$ in. at $p_\infty = 6$ cm Hg; $V_\infty = 15{,}000$ fps. Data compared with turbulent cone wake theory.

(which is dominated by large-scale structure) with the calculated results of Webb and Hromas[2, 3] which are based on a small-scale mixed turbulence model of the hypersonic cone wake. Lien et al.[4, 6]§ use the actual outline of the viscous core from schlieren photographs to specify the mixing parameters.

These considerations having been set forth, Fig. 3 compares the experimentally determined cone wake velocity in the turbulent core with the theoretical centerline velocity.[3, 6]¶ The Webb and Hromas calculation is begun with a laminar run of wake; the results are shown only for the turbulent part of the modeled flow field. The rms deviation value for the curve fit of the experimental data represents the statistical nature of the unsteady phenomenon being observed for three separate runs at 6.0 cm Hg. The important point is that the center of gravity of the experimental data falls meaningfully close to the theoretical calculation, both being significantly below the sphere results for the regime $x/d < 25$ (see Fig. 4).

All the wake velocity decay results for the 15° cone are shown in the form of quartic curve fits in Fig. 4. Since turbulent diffusion is dominated by geometric effects, once the mixing-length assumption ($\theta_{turbulent} \sim$ wake width times velocity defect) is valid, the results are not expected to be sensitive to freestream pressure. As the ballistic range pressure decreases, there will come a point where the energy in the

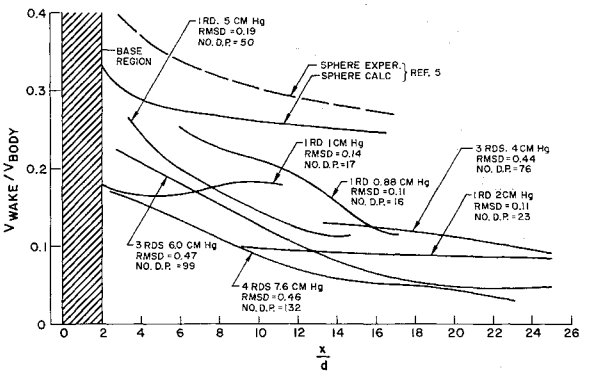

Fig. 4 Cone wake velocity data for 15° semivertex angle cones; $d_{base} = \frac{1}{2}$ in. at $p_\infty = 7.6$, 6.0, 5.0, 4.0, 2.0, 1.0, and 0.88 cm Hg, $V_\infty \approx 15{,}000$ fps. Number of data points (D.P.) and root-mean-square deviation (RMSD) for each curve are noted.

§ The body in the Lien calculation has twice the base diameter of the experimental model, but the results are expected to scale as d. The average cone wake velocity (denoted V_{avg} in Fig. 3) is

$$\int_0^1 V(\eta)d\eta$$

where η is the ratio y/y_{core}.

¶ All velocities are measured relative to a coordinate system fixed in the laboratory.

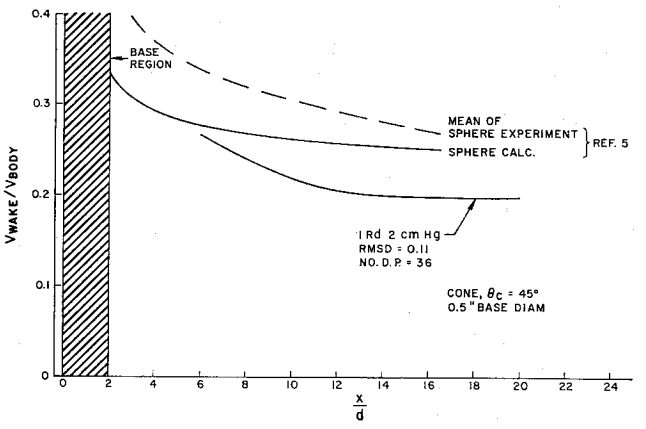

Fig. 5 Cone wake velocity data for a 45° semivertex angle cone; $d_{base} = \frac{1}{2}$ in., $p_\infty = 2$ cm Hg. Data compared with sphere wake results.

large-scale structure will not be sufficient to induce a turbulent growth of the wake, and a slower velocity decay tending toward the higher velocities of a theoretical laminar result is to be expected. Evidence of such an effect is somewhat suggested by the $P\infty = 0.88$ and 1-cm data in the experimental results presented in Fig. 4. It must be remembered that this suggestion is based mostly on a phenomenological expectation.

The unsteady wake phenomenon in the sphere experiments was observed as streaks in the same manner as just shown for the cone. However, the sphere calculation shown in Fig. 4 comes from an inviscid stream tube calculation. For spheres, the near-wake region $x/d < 15$ is dominated by the strong pressure decay. The large-scale unsteady structure in the viscous core is sucked into the expansion region, and consequently the velocity decay is being dominated by the pressure distribution set up by the shock-induced inviscid flow field rather than by turbulent diffusion.

A physical explanation as to why sphere wake velocities are higher than the cone wake velocities may be as follows. The sphere produces a relatively large-radius shock, thereby creating a large flux of high-velocity gas in and adjacent to the viscous core. In the slender cone case, $\theta_c \sim 15°$, the gas adjacent to the viscous core is of relatively low velocity (very nearly the ambient value) and hence more rapidly decelerates the viscous core gas via turbulent diffusion.

Experimental results for the 45° semivertex angle cone, $d_{base} = \frac{1}{2}$ in., do not fall along the slender cone theory line (Fig. 3) but come near to, although lower than, the sphere results (Fig. 5). The C_D shock drag for a 45° cone and for a sphere are approximately equal, both being close to one. However, the distribution of the momentum deposition in the gas behind the shock is somewhat different. In the sphere case, the deposition is nonuniform because of the large curvature of the bow shock. This gives rise to larger velocities at smaller radii and smaller velocities further out in the flow field. In the cone case, the shock is straight, the deposition is uniform, and the velocities at small radii are relatively less than those in the sphere case. Thus, in the case of the 45° cone relative to the sphere, the gas adjacent to the viscous core is of relatively lower velocity, hence decelerating the viscous core gases more rapidly via turbulent diffusion.

The region $x/d < 2$ has been crosshatched in Figs. 3–5 to indicate that the data cannot be reliably obtained this close to the base from the present streak photographs because of overexposure and rapid deceleration.

Slattery and Clay[1] measured wake velocities of 12.5° θ_c cones by following packages of density gradients in schlieren motion pictures from frame to frame. The initial values of V_{wake}/V_{body} determined by Slattery and Clay, $V_{wake}/V_{body} = 0.20$ at $x/d \approx 60$, are somewhat higher than the final value $V_{wake}/V_{body} \approx 0.1$ at $x/d = 22$ reported here. The difference is believed to be due to the relatively long shutter speed of the Fastax camera used for observing wake flow velocities in this region of the wake. The accuracy of their technique improves for $x/d > 100$, where the wake speeds are slower.[9]

References

[1] Slattery, R. E. and Clay, W. G., "The turbulent wake of hypersonic bodies," ARS Preprint 2673-62 (1962).

[2] Hromas, L. and Lees, L., "Effect of nose bluntness on the turbulent hypersonic wake," Space Technology Labs. Rept. 6130-6259-KU-000 (October 1962).

[3] Webb, W. H., private communication (September 1963).

[4] Lien, H., Erdos, J., and Pallone, A., "Nonequilibrium wakes with laminar and turbulent transport," AIAA Preprint 63-447 (1963).

[5] Hidalgo, H., Taylor, R. L., and Keck, J. C., "Transition in the viscous wake of blunt bodies at hypersonic speeds," Avco-Everett Research Lab. Res. Rept. 133 (April 1961); also J. Aerospace Sci. 29, 1306–1316 (1962).

[6] Lien, H., private communication (September 1963).

[7] Fay, J. and Goldburg, A., "Unsteady hypersonic wake behind blunt bodies," AIAA J. 1, 2264–2272 (1963); also "The unsteady hypersonic wake behind spheres," Avco-Everett Research Lab. Res. Rept. 139 (November 1962).

[8] Goldburg, A., "Analysis of hypersonic wake transition experiments," Avco-Everett Research Lab. Res. Rept. (to be published).

[9] Slattery, R., private communication (October 1963).

Pressure Gradients in a Liquid Propellant Rocket Motor

WILLIAM T. PESCHKE* AND SANFORD S. HAMMER†
Polytechnic Institute of Brooklyn, Farmingdale, N. Y.

Introduction

IN the design of liquid propellant rocket combustors it is desired to have complete burning take place within the combustion chamber. In addition, the liquid- and gasdynamic flow fields should be inherently stable. Recent investigations,[1, 2] based on a vaporization rate controlled combustion process, resulted in methods to determine the minimum chamber length required to insure complete combustion and the flow fields response to input disturbances. The theoretical analysis predicted mass liberation schedules, gas and droplet velocity histories, and axial pressure histories. It was found that increases in the mass liberation rate are accompanied by attendant increases in the magnitude of the pressure gradient with a corresponding increase in the velocity gradient. Initial experiments designed to measure axial pressure gradients were in good agreement with the theory for a given set of injection parameters.[1] In order to obtain correlation, it was necessary to assume a drop size distribution and a droplet formation distance, i.e., the required distance from the injector face for the injected ligaments to form a discrete droplet distribution. The analysis distinctly indicated that energy (mass) liberation gradients can be deduced from pressure gradient measurements. Thus, the chamber length for optimum propellant utilization and thrust production is related to the axial pressure gradient. In a motor whose geometry and propellant mass flow rate are fixed, this gradient

Received March 25, 1964; revision received May 1, 1964. The results obtained in this paper were obtained in the course of research sponsored by the Air Force Office of Scientific Research under Grant No. AF-AFOSR-86-63. The authors wish to acknowledge Vito D. Agosta for his helpful discussions.

* Research Assistant, Aerospace Engineering, Propulsion Research Laboratory. Member AIAA.

† Research Associate, Aerospace Engineering, Propulsion Research Laboratory. Member AIAA.